Journal of Sound and Vibration (2000) **238**(1), 31–49
doi:10.1006/jsvi.2000.3101, available online at http://www.idealibrary.com on IDEAL®

SPECTRAL CONDITIONING OF PROPELLER NOISE FROM BROADBAND SOURCES

M. Carley and J. A. Fitzpatrick

Department of Mechanical Engineering, Trinity College, Dublin 2, Ireland

(*Received* 7 *May* 1999, *and in final form* 8 *May* 2000)

The effect of turbulent loading on the noise radiated by an advanced aircraft propeller is assessed using a spectral conditioning technique which allows the inclusion of the non-linear effects associated with source rotation. The method allows the steady-source noise at a microphone to be estimated by removing the effect of measured on-blade unsteady loading. The operation of the method is demonstrated by using numerically simulated data, demonstrating the effectiveness of the technique in extracting the steady-source sound. Experimental results are presented showing the effect of random loading on the acoustic field of a propeller in an axial flow and at incidence. It is shown that, for the range of conditions and microphone positions considered, the effect of turbulent loading on the radiated noise can vary from about 2–8 dB, being stronger upstream than downstream.

1. INTRODUCTION

One of the main design drivers in modern aircraft design is noise reduction. Advanced propeller designs offer the possibility of increased fuel efficiency but only if the noise which they generate can be controlled to within the limits imposed by current regulations. Over the past 30 years, noise prediction methodology has improved markedly, beginning with the work of Ffowcs Williams and Hawkings [1] and continuing with the development of time-domain [2, 3] and frequency-domain [4] methods. These exact methods extend the knowledge of propeller noise gained from earlier work on the problem, due to Gutin [5] and Lowson [6], who developed point force methods in the frequency and time domains, respectively. All of the early prediction techniques could, in principle, be used to predict the noise associated with unsteady loading on the propeller blade but, initially, this was not the main concern. It was Wright [7] who initially analyzed this effect, in connection with helicopter rotor noise where loading fluctuations are of great importance. There is inevitably some unsteady loading on a propeller blade due to asymmetric inflow (angle of attack or wing interference, for example). When a propeller operates at incidence there is a further effect on the radiated noise from asymmetric radiation into the flow. This has been increasingly recognized in the work of Stuff [8], Mani [9] and Hanson [10]. At this stage, the effect of deterministic loading variations on a blade (steady and periodic) is well understood and can be predicted quite accurately. In this work, the effect of random loading variations is studied.

Assessment of the noise radiated by random variations is a difficult task, in part because of the difficulty of predicting the turbulent pressures which constitute the acoustic source term. The effect of turbulence on propeller noise depends on the baseline turbulence of

0022-460X/00/460031 + 19 $35.00/0

the atmosphere in flight and on how that turbulence is affected by ingestion into the propeller flow field. Analytical prediction of the noise generated by turbulence ingestion into propellers and fans can be found in the work of Majumdar and Peake [11], who considered the important question of the differences between static testing and flight conditions, in the work of Amiet *et al.* [12], who made noise predictions incorporating the effect of distorted atmospheric turbulence and Aston *et al.* [13] who compared theoretical results with experimental data for a ducted rotor at low Mach number. In this work, it was found that the dominant factor in the radiated noise due to ingested turbulence was the form of the turbulence spectrum. Similarly, Majumdar and Peake [11] found that the radiated noise was sensitive to the turbulence parameters and in particular to the integral length scale.

In the work presented here, the effect of broadband sources is studied by using a combination of theoretical modelling and a signal-conditioning technique which incorporates the known acoustic system parameters. The approach is akin to that of Visintainer *et al.* [14], who predicted the noise radiated from a helicopter rotor by using measured blade pressures. In the study presented here, however, the objective is to estimate the contribution of the broadband blade pressure (however it may have been generated) to the farfield noise spectra, using on-blade and acoustic measurements. This requires the development of a physical model for the system and the development of a procedure which uses the results from this model. These are developed in the next two sections and the results from experimental testing are given in section 5.

2. CONDITIONING METHOD

The method used to estimate the contribution of broadband sources to the radiated noise is a general spectral conditioning technique developed by Bendat and Piersol [15] and applied, for example, by Esmonde *et al.* [16]. A schematic of the general system is shown in Figure 1. The inputs to the system l_i are the on-blade fluctuating pressures measured at discrete points. Each of these inputs passes through a non-linear operator g_i which models the effect of radiation from a rotating source; this operator will be defined in section 3. The output of the system $p'(t)$ is the sum of the broadband signals after "rotation", the underlying deterministic signal $x(t)$ and any extraneous noise $n(t)$. The objective of the conditioning procedure is to estimate and remove from the output acoustic spectrum

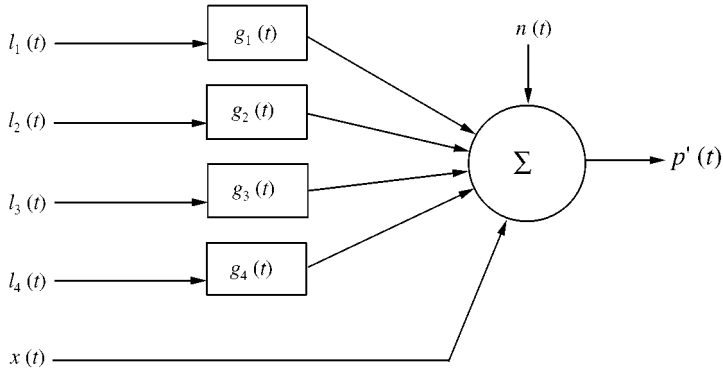

Figure 1. Input/output model for propeller noise.

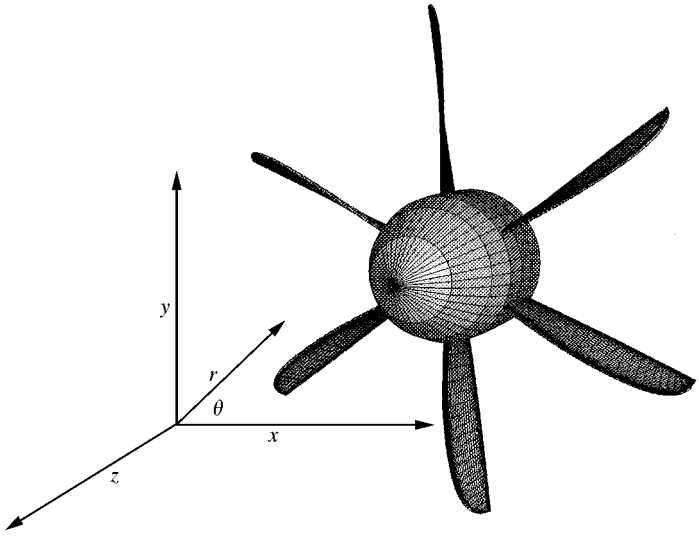

Figure 2. Geometry of physical system.

the noise due to the broadband inputs. It should be noted that the system being conditioned is linear. The inputs are passed through their non-linear operators before the conditioning procedure is applied. The output of the system is a linear combination of the inputs, making the conditioning procedure applied here a valid approach.

The geometry of the physical system is shown in Figure 2.

2.1. CONDITIONING PROCEDURE

The method used to condition the measured acoustic spectra is based on a partial coherence method previously applied to a number of systems [16, 17]. The first step is to calculate the acoustic signal due to each broadband source, by using the model of section 3. This is accomplished by subtracting from the output spectrum that part of each input spectrum which is correlated with it, first having conditioned the inputs so that they are uncorrelated with each other. The system is shown in Figure 3 with $u_i(t)$ being the unsteady-source contribution in the time domain, $x(t)$ the (unknown) deterministic component and $p(t)$ the microphone signal. The extraneous noise is $n(t)$. For uncorrelated inputs, the contribution of input i to the output spectrum is the coherence function

$$\gamma_{ip}^2(f) = |G_{ip}(f)|^2 / G_{ii}(f) G_{pp}(f)$$

where $G_{pp}(f)$ is the autospectrum of $p(t)$ and $G_{ii}(f)$ is the autospectrum of $u_i(t)$. The contribution of the ith source can then be removed by subtracting the correlated part:

$$G_{pp.i} = (1 - \gamma_{ip}^2) G_{pp}.$$

The notation $G_{pp.i}$ signifies G_{pp} conditioned with respect to the ith input. If the inputs are uncorrelated, this procedure can be applied to each input in turn. In practice, however, the

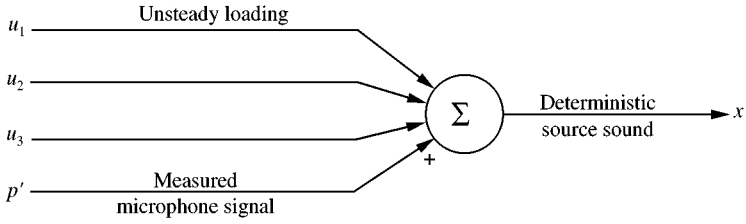

Figure 3. Modified input/output system.

inputs are correlated and so must be conditioned with respect to each other to generate a set of uncorrelated inputs.

This conditioning is performed by sequentially conditioning out one record $u_i(t)$ at a time, by using the recursion relation

$$G_{pp.i} = (1 - \gamma^2_{ip.(i-1)!})G_{pp.(i-1)!},$$

where $\gamma^2_{ip.(i-1)!}$ is the partial coherence

$$\gamma^2_{ip.(i-1)!} = |G_{ip.(i-1)!}|/G_{ii.(i-1)!}G_{pp.(i-1)!}$$

and the residual auto-spectra and cross-spectra are given by

$$G_{jk.r!} = G_{jk.(r-1)!} - L_{rj}G_{jr.(r-1)!}$$

with L_{rj} being the conditioned frequency response function

$$L_{rj} = G_{rj.(r-1)!}/G_{rr.(r-1)!}.$$

To monitor how strongly the microphone spectrum has been conditioned, the multiple coherence is used. This gives a measure of the correlation between the current conditioned spectrum and the conditioned inputs:

$$\gamma^2_m = 1 - \prod_{i=1}^{n} (1 - \gamma^2_{ij}).$$

2.2. IMPLEMENTATION

The procedures of the previous section were applied in essentially the sequence described above. Starting with the signals from the on-blade Kulite pressure transducers, the sequence is as follows: (1) remove mean level from Kulite records $l_i(t)$; (2) notch filter $l_i(t)$ to remove the periodic loading contribution; (3) calculate $u_i(t)$ from unsteady pressure data $l_i(t)$ by using equation (2); (4) compute spectra and cross-spectra for $u_i(t)$ and $p(t)$; (5) sequentially condition microphone spectrum $G_p(f)$ to eliminate $G_u(f)$.

The only difficulty arises in step (5) where singularities can be encountered when the spectrum has been completely conditioned. This was avoided by terminating the procedure when the multiple coherence exceeded a specific value, set at 0·95.

The notch filtering in step (2) is performed to remove the periodic, deterministic contribution to the on-blade pressure. The component of loading at integer multiples of the propeller rotation frequency was removed, so that only the turbulent contribution remained.

3. PHYSICAL MODEL

To implement the conditioning procedure of section 2.1, the noise radiation process must be modelled in a manner which allows the generation of inputs for the procedure. The requirement is for a model which calculates the time-domain acoustic signal associated with the time-domain blade-pressure record. This is a non-linear process but one which can be modelled exactly. The noise generated by a propeller is related to its geometry and to the on-blade pressure, quadrupole sources being negligible for the thin, highly swept blades used in this study [18]. A model based on linear acoustic theory is used which incorporates unsteady loading and asymmetric convection. The first of these is obviously essential: turbulence is an unsteady effect and a steady-loading model would be unable to give any information about the radiated noise due to unsteady-loading sources. The second feature, asymmetric inflow, is needed to allow incidence effects to be modelled correctly.

The noise model used was developed for noise prediction and has been validated against experimental data [19]. For a propeller operating in a subsonic flow of velocity cM_∞ with a surface distribution of $\mathbf{l}$ force per unit area

$$4\pi p'_L = \frac{1}{c}\int_S \left[\frac{1}{1-\mathbf{M}_s\cdot\mathbf{D}}\frac{\mathrm{d}}{\mathrm{d}\tau}\left(\frac{\mathbf{l}\cdot\mathbf{D}}{R(1-\mathbf{M}_s\cdot\mathbf{D})}\right)\right]_{g=0}\mathrm{d}S + \int_S \left[\frac{\mathbf{l}}{R(1-\mathbf{M}_s\cdot\mathbf{D})}\left(\frac{\mathbf{R}}{R}-\frac{\dot{\mathbf{R}}}{c(1-\mathbf{M}_s\cdot\mathbf{D})}\right)\right]_{g=0}\mathrm{d}S, \tag{1}$$

where

$$g = \tau - t + (R - \mathbf{M}_\infty\cdot(\mathbf{x}-\mathbf{y}))/\beta^2 c,$$

$$R = (\beta^2|\mathbf{x}-\mathbf{y}|^2 + [\mathbf{M}_\infty\cdot(\mathbf{x}-\mathbf{y})]^2)^{1/2},$$

$$\beta^2 = 1 - |\mathbf{M}_\infty|^2, \qquad \mathbf{M}_s = \dot{\mathbf{y}}/c, \qquad \mathbf{R} = \nabla R,$$

$$\mathbf{D} = \frac{\mathbf{R}}{\beta^2} - \frac{\mathbf{M}_\infty\cdot(\mathbf{x}-\mathbf{y})}{\beta^2}(\mathbf{x}-\mathbf{y}).$$

Here S is the blade surface with $\mathbf{x}$ and $\mathbf{y}$ being observer and source co-ordinates respectively. The acoustic source associated with $\mathbf{l}$ on the blade surface has a dipole directivity with the dipole axis directed along the normal to the blade surface. The terms of equation (1) can easily be adapted to predict the noise generated by a point force moving in a flow,

$$4\pi p'_L = \frac{1}{c}\left[\frac{1}{1-\mathbf{M}_s\cdot\mathbf{D}}\frac{\mathrm{d}}{\mathrm{d}\tau}\left(\frac{\mathbf{l}\cdot\mathbf{D}}{R(1-\mathbf{M}_s\cdot\mathbf{D})}\right)\right]_{g=0} + \left[\frac{\mathbf{l}}{R(1-\mathbf{M}_s\cdot\mathbf{D})}\left(\frac{\mathbf{R}}{R}-\frac{\dot{\mathbf{R}}}{c(1-\mathbf{M}_s\cdot\mathbf{D})}\right)\right]_{g=0}, \tag{2}$$

where $\mathbf{l}$ is now a point force. By using equation (2), the noise radiated to a known microphone position $\mathbf{x}$ by a rotating source at position $\mathbf{y}(t)$ with strength $\mathbf{l}(t)$ can be calculated. For a given on-blade transducer, the position is known and the force signal is one of the experimental measurements. The acoustic signal is measured at $\mathbf{x}$ so that all of the information needed for the application of the technique of section 2 is available.

4. EXPERIMENTAL TESTS

The propeller tested was a high-speed, wide-chord design with a highly swept blade. The tests were performed at Mach number $M = 0{\cdot}2$ on a model propeller at the DNW open-jet facility in the Netherlands and included inflow incidence conditions in which unsteady phenomena were expected to contribute substantially to the noise generated. Instrumentation on the blades consisted of steady pressure tappings and 36 Kulite-type transducers to monitor unsteady blade pressures while microphone arrays were used to measure the near- and farfield noise. Acoustic measurements were performed on sidelines at fixed radius from the propeller axis. The locations of the Kulite transducers on the blade suction surface are shown in Figure 4(a) and on the pressure surface in Figure 4(b). The data were acquired at 16 kHz and stored as time-domain records for subsequent data processing. The tests were part of a series carried out under the EC-funded research programme Study

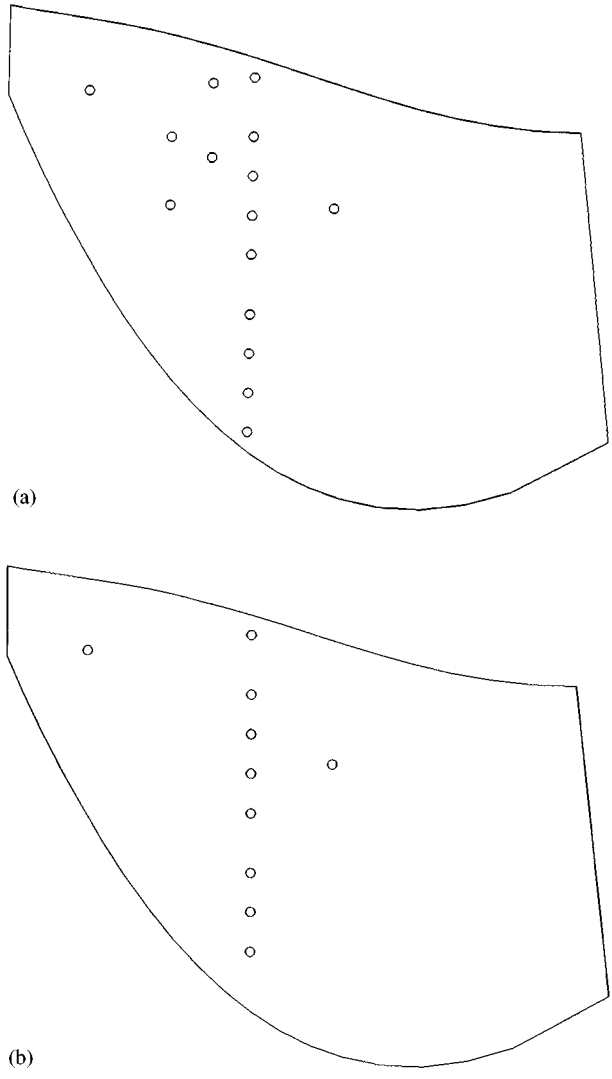

Figure 4. Test blades and Kulite positions.

of Noise and Aerodynamics of Advanced Propellers (SNAAP). The objective of the work was to develop and validate an integrated code for propeller noise predictions.

The conditioning procedure was applied to farfield microphone data taken on a sideline 5·53 blade radii from the propeller axis. The propeller was operated at 4750 rpm in a flow of Mach number 0·2 and at angles of attack 0, 5, 10 and 15°.

5. RESULTS

The results from the Kulite transducers and from the field microphones were recorded as time records and the analysis was implemented as detailed in section 3.3. Auto- and cross-spectra were obtained from 25 averages of 1024 point transforms. The frequency range was from 0 to 8192 Hz with a resolution of 16 Hz.

5.1. NUMERICAL SIMULATION

To check that the conditioning procedure worked correctly, it was tested by numerically simulating the noise radiated by three rotating sources, one steady and two broadband with superimposed periodic contributions. The r.m.s. value of the sound radiated by the broadband signals was 2·8 times the r.m.s. value of the sound radiated by the deterministic terms. The objective was to recover the spectrum due to the periodic and steady sources through application of the procedure of section 2.1. The two broadband sources were uncorrelated and at different positions from each other and from the periodic source. There are three signals to consider: $G(f)$, the "measured" spectrum, made up of the sum of the deterministic and the random source signals; $G_c(f)$, the signal generated by conditioning $G(f)$ with respect to the "rotated" random source signals; $G_r(f)$, the reference spectrum which is the spectrum of the deterministic source signal only. The technique is assessed by how close G_c is to G_r. To emphasize the differences between spectra, their ratio to G_r is shown. Figure 5 shows the ratio of the spectra before conditioning, i.e., G/G_r. The ratio is shown in two forms, the first (Figure 5(a)) is the ratio shown over the whole spectrum, while the second (Figure 5(b)), shows the ratio at the harmonics of the rotation frequency. In the full spectrum case, the effect of the broadband sources is a large increase in the amplitude of the spectrum between the harmonics. The amplitude of the harmonics, shown in Figure 5(b), increases markedly however.

Figure 6 shows the ratio of the conditioned and reference spectra after the conditioning procedure has been applied. The scale of the graph is much smaller and the large differences seen in Figure 5 have disappeared. The broadband noise at the off-harmonic frequencies has been eliminated, despite being from 20 to 80 dB higher than the power in the reference spectrum. Furthermore, an examination of the ratio of G_c/G_r at the harmonics of the rotation frequency, Figure 6(b) reveals that the first 20 harmonics of the conditioned signal are within 1 dB of the corresponding values of the reference spectrum. On the basis of the simulated results, it is possible to have confidence in the results presented in section 5.3.

5.2. UNSTEADY BLADE PRESSURE SPECTRA

Typical auto-spectra from a Kulite for these tests are shown in Figure 7. Like all the experimental results presented in this paper, an arbitrary reference has been used for normalization in calculating dB level. For zero incidence, it can be seen from Figure 7(a) that the spectrum has two dominant peaks, the first at the blade rotational speed and the

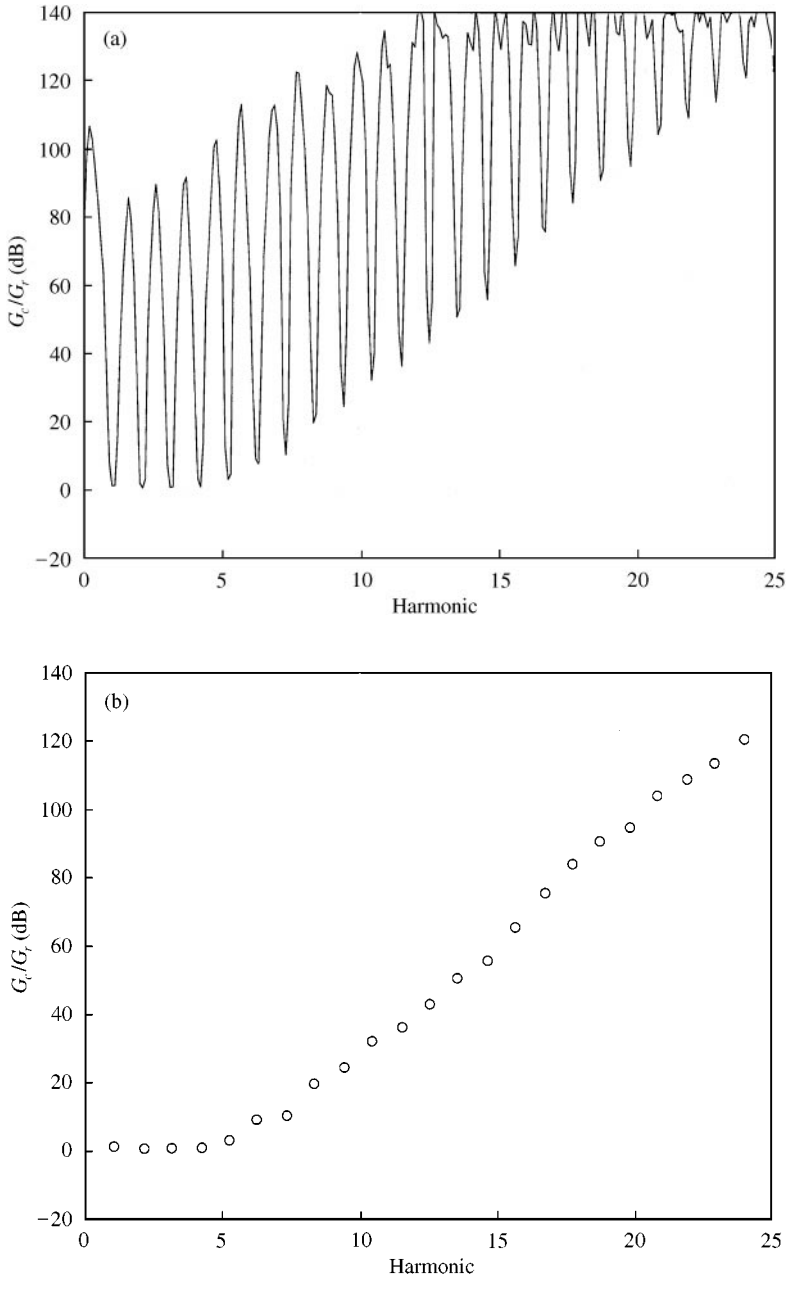

Figure 5. Ratio of simulated unconditioned and reference spectra (a) Full spectrum; (b) harmonics only.

second at twice this value. The other peaks in the spectrum at higher harmonics of the rotational speed are 15 dB below these two. At 5° incidence (Figure 7(b)), the peak at the rotational speed is now dominant and has increased by nearly 20 dB above the zero incidence level. It is 15 dB above the second harmonic and 25 dB greater than the higher harmonics. In Figure 7(c), for 10° incidence, the peak has increased again by 5 dB as has the second harmonic whilst the remaining harmonics are at the same level. Finally, at 15°,

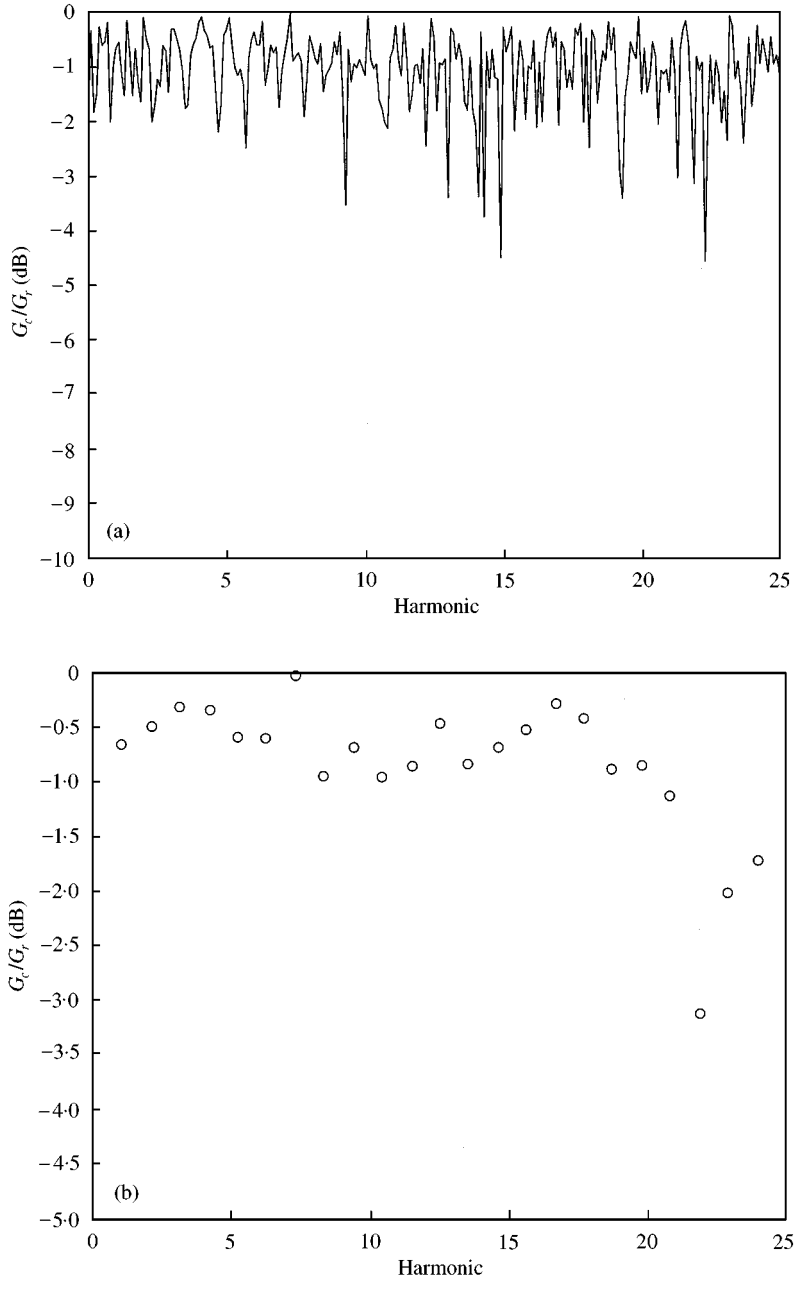

Figure 6. Ratio of simulated conditioned and reference spectra (a) Full spectrum; (b) harmonics only.

a further increase of 5 dB is evident at the fundamental frequency and some 6 dB at the second harmonic as can be seen from Figure 7(d). Thus, from 0° of incidence to 15°, the unsteady pressure peak has increased by 25 dB. The effect of incidence then is to greatly increase the unsteady pressure fluctuation especially at the blade rotational speed and this would be expected to alter substantially the character of the radiated noise [7].

5.3. CONDITIONED MICROPHONE SPECTRA

Figure 8 shows the conditioned and unconditioned spectra in the propeller plane for the four angles of incidence considered. In each case, the conditioned spectrum is indicated by a circle at the harmonics of the blade passage frequency. The most visible effect of conditioning is the reduction in the broadband noise by about 3 dB across the range.

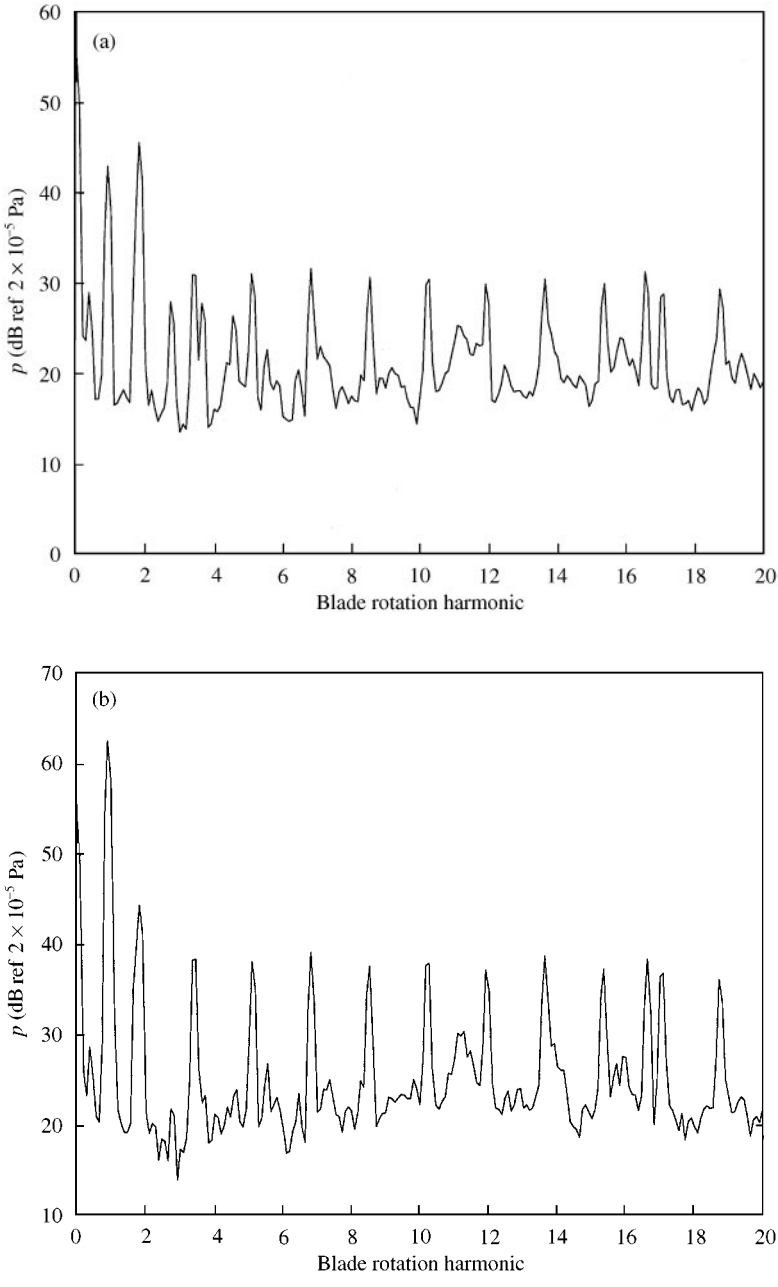

Figure 7. Measured Kulite spectra. $M = 0{\cdot}2$. (a) $\alpha = 0°$; (b) $\alpha = 5°$; (c) $\alpha = 10°$; (d) $\alpha = 15°$.

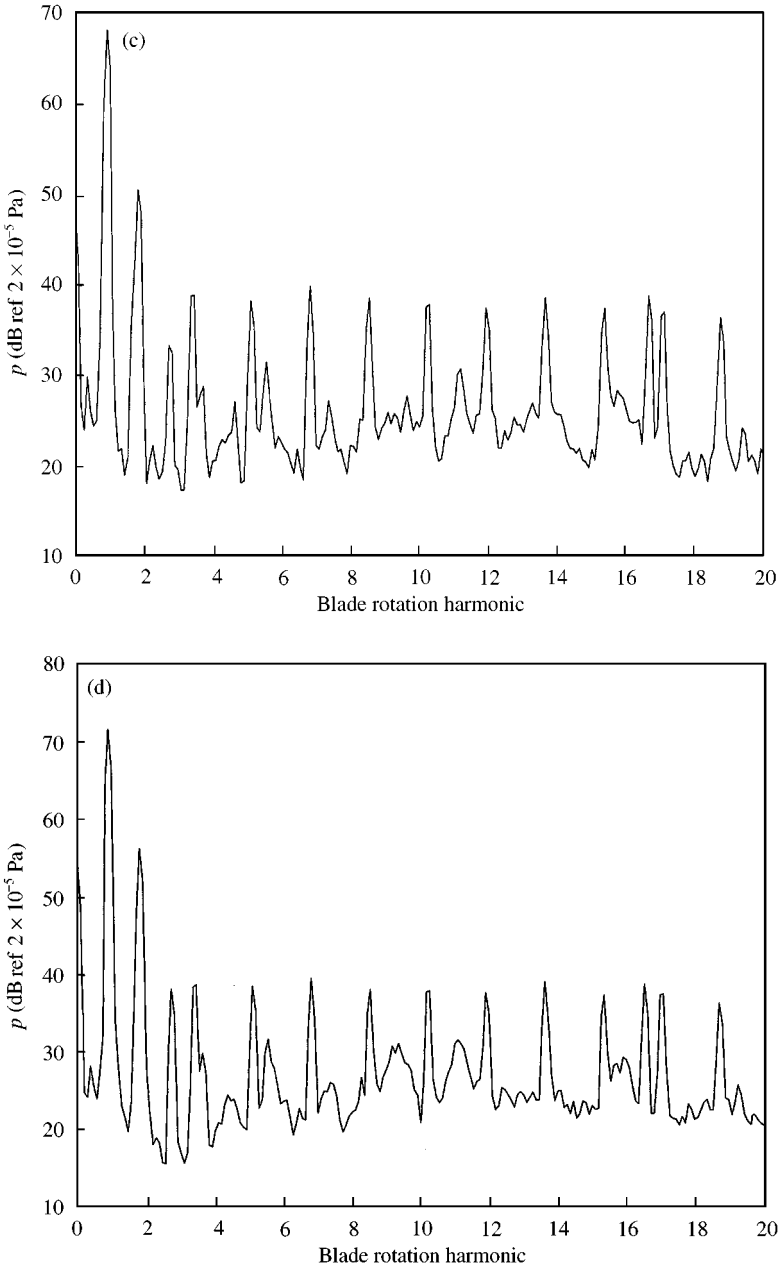

Figure 7. Continued.

A large reduction in the broadband noise is not to be expected, as most of the energy in the turbulent-source spectrum is radiated at the harmonic frequencies but there will be some effect, as seen in the numerically simulated data (Figure 6). Figures 9 and 10 show the conditioned and unconditioned directivities on the sideline for the first and second harmonics of the radiated noise, respectively, for each of the angles of attack. In the directivity plots, three curves are shown: the conditioned harmonic strength, the unconditioned harmonic strength and, as a reference, the conditioned spectrum for $\alpha = 0^\circ$.

For the first harmonic, (Figure 9) the effect of the random loading is of the order of 3–4 dB at zero incidence (Figure 9(a)) although it is rather higher at large values of z, where the radiated field is weaker. As the angle of attack is increased, the effect of random loading becomes greater and the conditioned directivity begins to drop below the conditioned 0° value upstream of the propeller ($z > 0$). In part, this effect may be due to the tilting of the propeller directivity field at incidence, a first order effect discussed by Campos [20], but

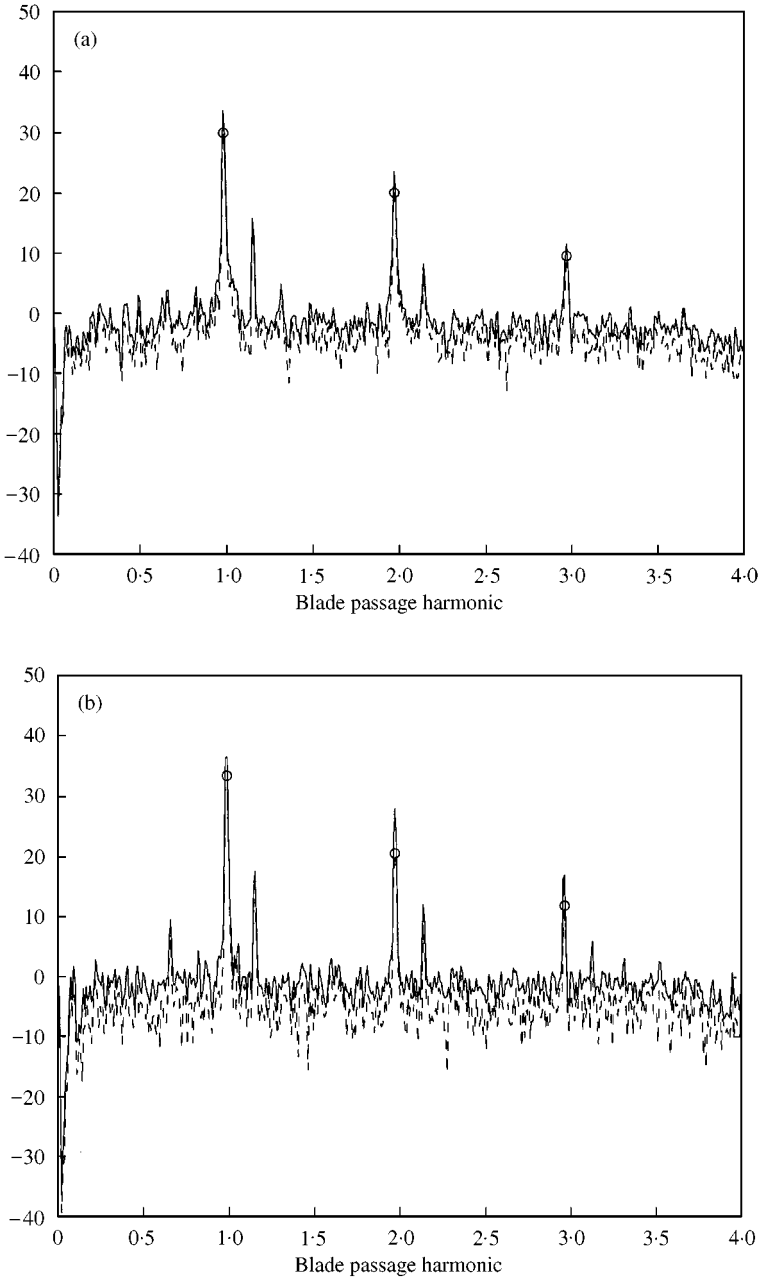

Figure 8. Measured and conditioned spectra. $M = 0{\cdot}2$. (a) $\alpha = 0°$; (b) $\alpha = 5°$; (c) $\alpha = 10°$; (d) $\alpha = 15°$. Values of conditioned spectra at harmonics indicated by circles.

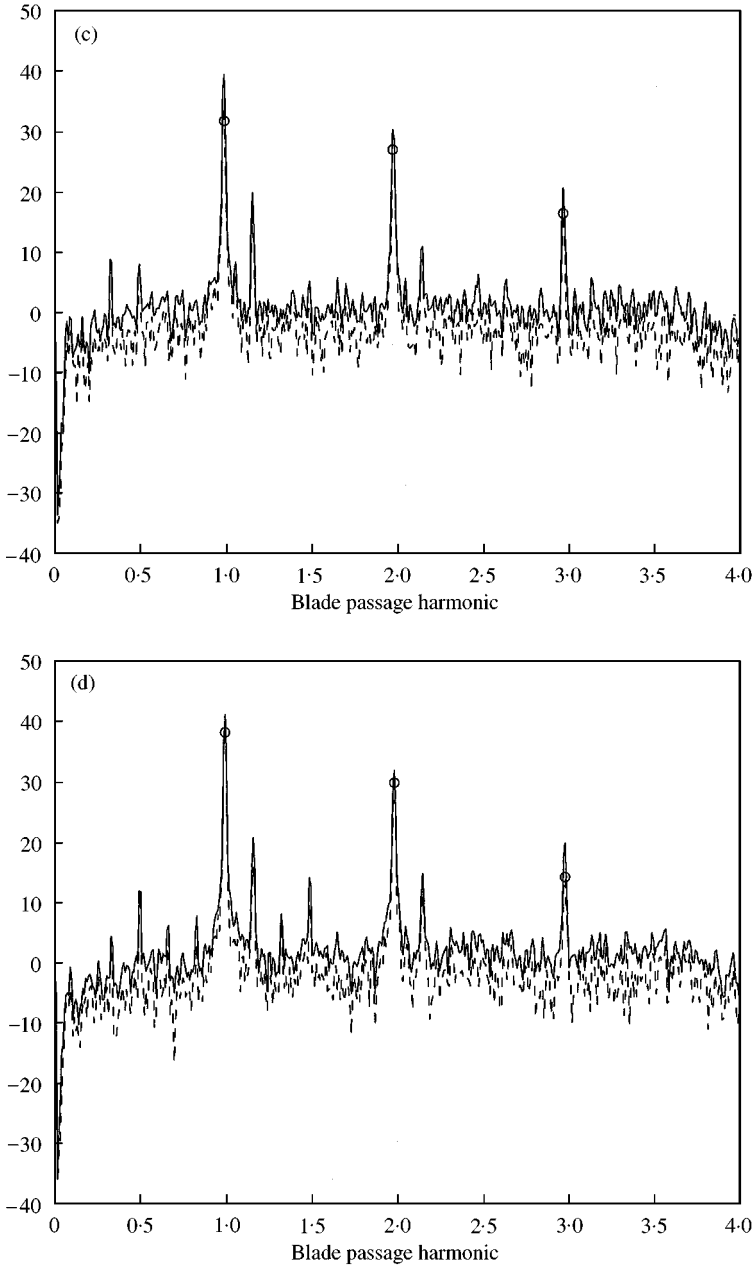

Figure 8. Continued.

there is also an effect from the increased fluctuating loading at higher incidence. Similarly, in Figure 10, showing equivalent data for the second harmonic, there is a strong effect of turbulent loading on the conditioned spectra. Looking at the extreme cases, $\alpha = 0^\circ$ and 15° (Figures 10(a) and 10(d) respectively) there is a large difference between the two directivities downstream of the propeller ($z > 0$) in both the conditioned and unconditioned cases. Upstream of the propeller ($z < 0$), the difference is much smaller, dropping to less than 1 dB at one point.

There appear to be two processes at work in the directivity results shown here. The first is the effect of tilting the directivity pattern of the propeller noise as incidence is increased. This tends to reduce the noise radiated to points on the sideline ahead of the propeller ($z < 0$) and increase the downstream noise. Part of this effect can be seen in the unconditioned data where, for example, the 0 and 15° directivities are very close, especially at large negative z. Downstream of the propeller disc, both the conditioned and

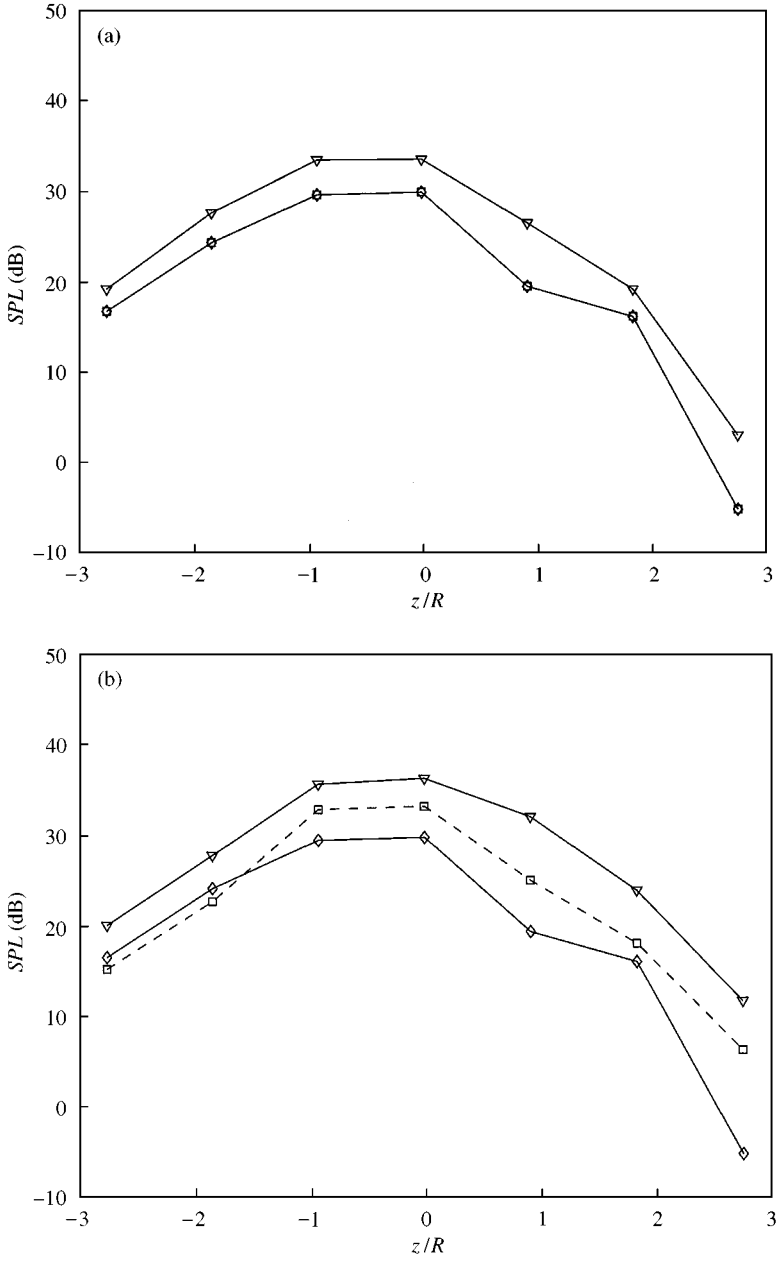

Figure 9. Axial directivity at blade pass frequency. $M = 0{\cdot}2$. (a) $\alpha = 0°$; (b) $\alpha = 5°$; (c) $\alpha = 10°$; (d) $\alpha = 15°$; △, unconditioned data; □, conditioned data; ◇, reference case, $\alpha = 0°$.

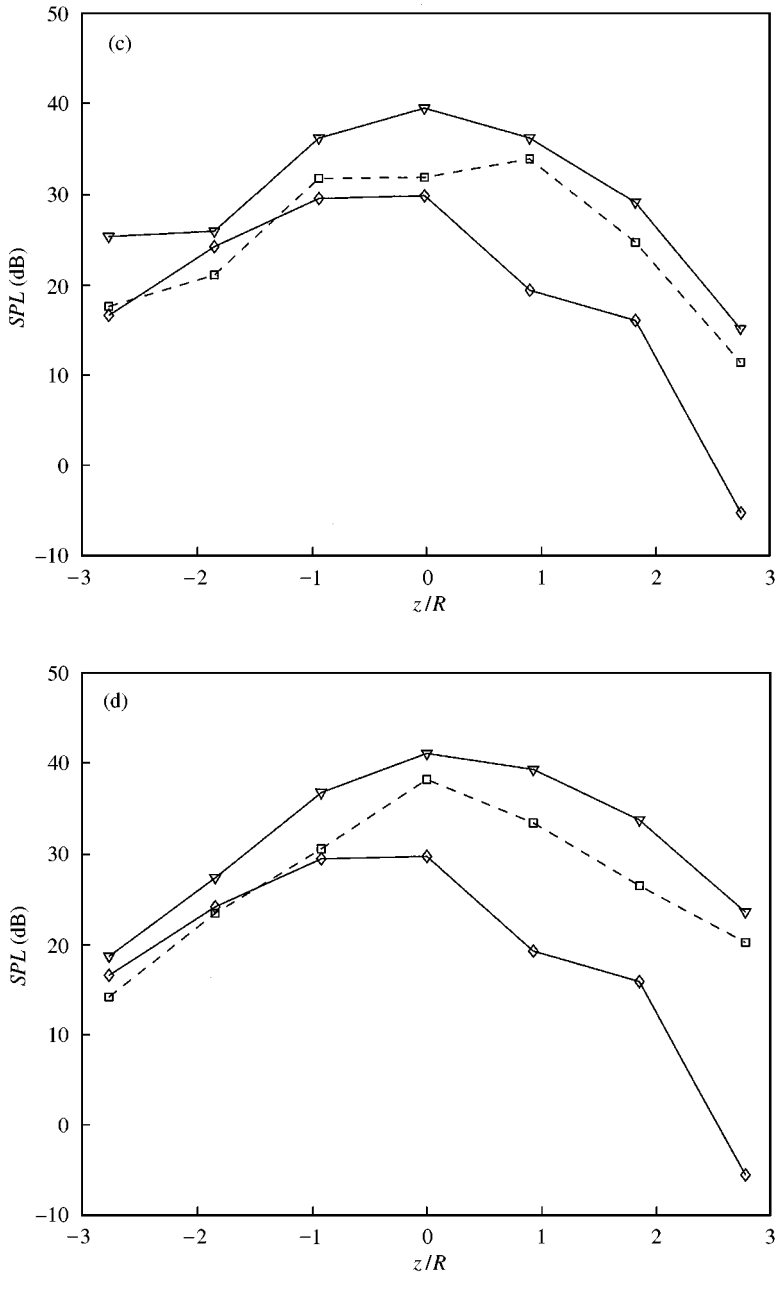

Figure 9. Continued.

unconditioned spectra are quite different. This appears to be due in part to the second effect of turbulent loading on the noise: changes in turbulent loading with incidence. Since the directivity is swept downstream by the inflow [21], noise due to additional loading tends to radiate preferentially to points at $z > 0$.

For the second harmonic directivities, (Figure 10), the broad trends are similar to those for the first harmonic, but with some differences in detail. Again, the conditioned

directivities are similar upstream of the disc, but in this case at higher incidence (Figures 10(c) and 10(d)), the directivities flatten out at the higher upstream values of z, although they dip slightly below the $\alpha = 0^\circ$ case near $z = -2$. Downstream of the propeller, it is the $\alpha = 0^\circ$ curve which shows the flattening and the higher incidence data which fall away continuously. This appears to be an effect of the tilting of the directivities mentioned above. The conditioned data at higher incidence are also much higher than the reference results

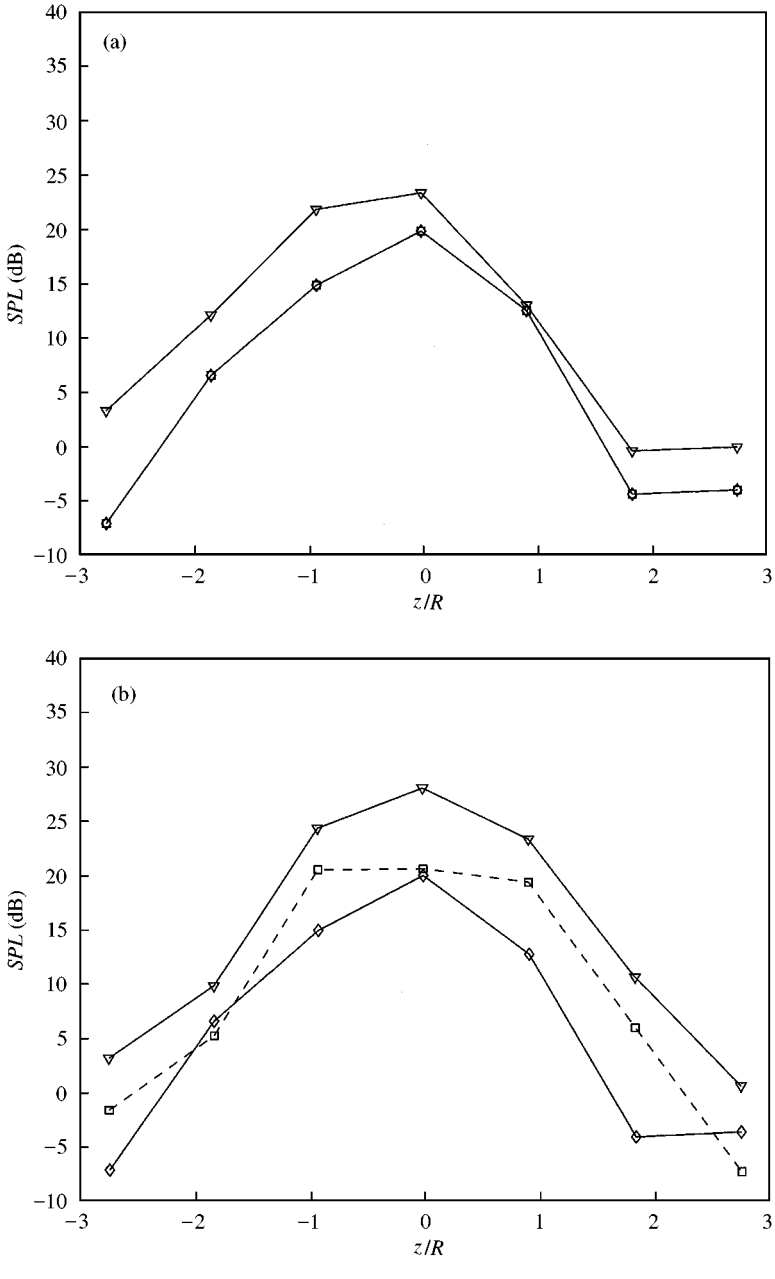

Figure 10. Axial directivity at second harmonic of blade pass frequency. $M = 0{\cdot}2$. (a) $\alpha = 0^\circ$; (b) $\alpha = 5^\circ$; (c) $\alpha = 10^\circ$; (d) $\alpha = 15^\circ$; $\triangle$, unconditioned data; $\square$, conditioned data; $\diamond$, reference case, $\alpha = 0^\circ$.

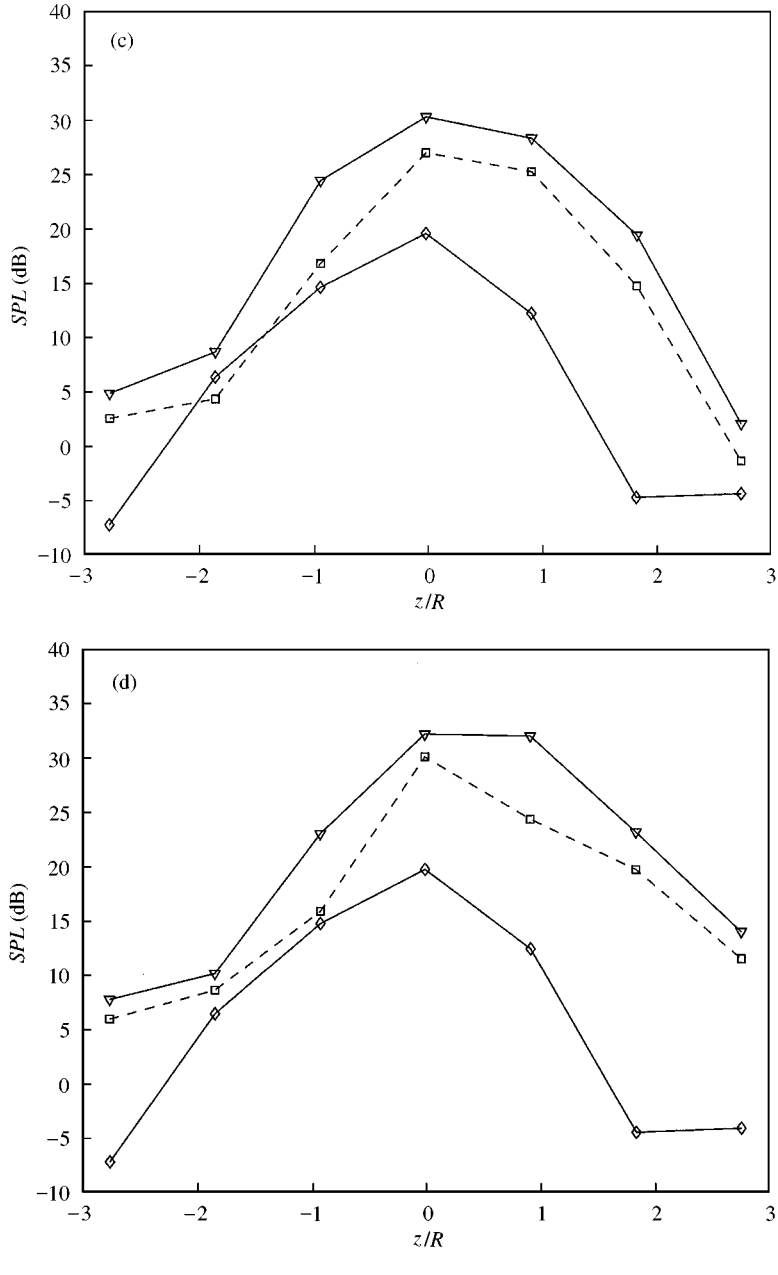

Figure 10. Continued.

downstream of the propeller. As in the first harmonic data, this may be due to preferential radiation of loading noise downstream; there is simply more turbulent-source noise downstream than there is upstream.

6. CONCLUSIONS

An established spectral conditioning procedure has been applied to the analysis of noise radiated by turbulent loading on an advanced high-speed propeller. The technique is based

on an established procedure for the conditioning of non-linear systems combined with a model of the acoustic radiation process for sources rotating in a uniform flow. The method has been tested by using numerical simulations and shown to be robust. The results indicate that the effect of turbulent loading in a wind tunnel test can vary from about 2 to 8 dB, depending on the microphone position and on the propeller incidence. The results appear to indicate that the noise associated with turbulent loading is stronger in the upstream than in the downstream direction and that there is an increase of about 3 dB in the broadband noise for the test conditions studied here. Finally, the processing method developed in this paper should be of some interest in developing improved theories of noise due to turbulence ingestion by propellers and fans, especially as regards the directivity of such noise.

ACKNOWLEDGMENT

The experimental data reported in this paper were obtained from the European Community project Study of Noise and Aerodynamics of Advanced Propellers (SNAAP). The authors wish to acknowledge the source of the data and the support of the European Commission under contract number AERO-CT92-0038.

REFERENCES

1. J. E. Ffowcs Williams and D. L. Hawkings 1969 *Philosophical Transactions of the Royal Society of London A* **264**, 321–342. Sound generation by turbulence and surfaces in arbitrary motion.
2. F. Farassat 1981 *AIAA Journal* **19**, 1122–1130. Linear acoustic formulas for calculation of rotating blade noise.
3. F. Farassat 1985 *Aerodynamics and Acoustics of Propellers, Paris*, Vol. 10. AGARD. Theoretical analysis of linearized acoustics and aerodynamics of advanced supersonic propellers.
4. D. B. Hanson 1985 *AIAA Journal* **23**, 499–504. Near-field frequency-domain theory for propeller noise.
5. L. Gutin 1948 *Technical Memorandum* 1195, *NACA, Langley Aeronautical Laboratory, Langley Field, VA, U.S.A.* On the sound field of a rotating propeller.
6. M. V. Lowson 1965 *Proceedings of the Royal Society of London A* **286**, 559–572. The sound field for singularities in motion.
7. S. E. Wright 1969 *Journal of Sound and Vibration* **9**, 223–240. Sound radiation from a lifting rotor generated by asymmetric disk loading.
8. R. Stuff 1988 *AIAA Journal* **26**, 777–782. Noise field of a propeller with angular inflow.
9. R. Mani 1990 *Proceedings of the Royal Society of London A* **431**, 203–218. The radiation of sound from a propeller at angle of attack
10. D. B. Hanson 1995 *Proceedings of the Royal Society of London A* **449**, 315–328. Sound from a propeller at angle of attack: A new theoretical viewpoint.
11. S. J. Majumdar and N. Peake 1998 *Journal of Fluid Mechanics* **359**, 181–216. Noise generation by the interaction between ingested turbulence and a rotating fan.
12. R. K. Amiet, J. C. Simonich and R. H. Schlinker 1990 *Journal of Aircraft* **27**, 15–22. Rotor noise due to atmospheric turbulence ingestion—Part II: aeroacoustic results.
13. J. A. G. Aston, C. J. Jenkins and J. Patmore 1996 *Proceedings of the 2nd AIAA/CEAS Aeroacoustics Conference, State College, PA, U.S.A., AIAA/CEAS*. An experimental investigation of broadband noise production from a large scale model ducted rotor.
14. J. A. Visintainer, M. A. Marcolini, C. L. Burley and Sandy R. Liu 1993 *Journal of the American Helicopter Society* **38**, 35–44. Acoustic predictions using measured pressures from a model rotor in the DNW.
15. J. S. Bendat and A. G. Piersol 1986 *Random Data: Analysis and Measurement Procedures*. New York: Wiley.
16. H. W. Esmonde, J. A. Fitzpatrick, H. J. Rice, and F. Axisa. *Proceedings of the IMechE* **206**, 225–238. Reduced order modelling of non-linear squeeze film dynamics.

17. C. MESKELL and J. A. FITZPATRICK 1995 *Flow-Induced Vibrations* 545–555, 6*th International Conference on Flow-Induced Vibration*. Validation of non-linear models for flow structure interaction.
18. D. B. HANSON and M. R. FINK 1979 *Journal of Sound and Vibration* **62**, 19–38. The importance of quadrupole sources in prediction of transonic tip speed propeller noise.
19. M. CARLEY 1986 *Ph.D. Thesis, Trinity College, Dublin* 2, *Ireland*. Time domain calculation of noise generated by a propeller in a flow.
20. L. M. B. C. CAMPOS 1999 *ASME Journal of Vibration and Acoustics* **121**, 50–58. On the influence of angle-of-attack or sideslip on far-field propeller noise.
21. M. CARLEY 1999 *Journal of Sound and Vibration* **225**, 353–374. Sound radiation from propellers in forward flight.